

Alma Mater Studiorum Università di Bologna
Archivio istituzionale della ricerca

Recyclable GO-Arginine Hybrids for CO₂ Fixation into Cyclic Carbonates

This is the final peer-reviewed author's accepted manuscript (postprint) of the following publication:

Published Version:

Angela Pintus, S.M. (2022). Recyclable GO-Arginine Hybrids for CO₂ Fixation into Cyclic Carbonates. CHEMISTRY-A EUROPEAN JOURNAL, 29, 1-6 [10.1002/chem.202202440].

Availability:

This version is available at: <https://hdl.handle.net/11585/913179> since: 2024-02-08

Published:

DOI: <http://doi.org/10.1002/chem.202202440>

Terms of use:

Some rights reserved. The terms and conditions for the reuse of this version of the manuscript are specified in the publishing policy. For all terms of use and more information see the publisher's website.

This item was downloaded from IRIS Università di Bologna (<https://cris.unibo.it/>).
When citing, please refer to the published version.

(Article begins on next page)

Recyclable GO-Arginine Hybrids for CO₂ Fixation into Cyclic Carbonates

Angela Pintus,^{[a]‡} Sebastiano Mantovani,^{[a]‡} Alessandro Kovtun,^[a] Giulio Bertuzzi,^[b,c] Manuela Melucci^{*[a]} and Marco Bandini^{*[b,c]}

[a] A. Pintus, S. Mantovani, A. Kovtun, Dr. M. Melucci
Istituto per la Sintesi Organica e Fotoreattività (ISOF) - CNR,
Via Gobetti 101, 40129 Bologna, Italy
E-mail: manuela.melucci@isof.cnr.it

[b] Dr. G. Bertuzzi, Prof. M. Bandini
Dipartimento di Chimica, "Giacomo Ciamician"
Alma Mater Studiorum – Università di Bologna
via Selmi 2, 40126 Bologna, Italy

[c] Dr. G. Bertuzzi, Prof. M. Bandini
Center for Chemical Catalysis – C³
Alma Mater Studiorum – Università di Bologna
via Selmi 2, 40126 Bologna, Italy

‡ These authors contributed equally.

Supporting information for this article is given via a link at the end of the document.

Abstract: New covalently modified GO-guanidine materials are realized on a gram-scale synthesis and purified via an innovative microfiltration. The use of these composites in the fixation of CO₂ into cyclic carbonates is demonstrated. Mild operating conditions, high yields (up to 85%), wide scope (15 examples) and recoverability/reusability (up to 5 cycle) of the material account for the efficiency of the protocol. Dedicated control experiments contributed to shed light on the activation modes exerted by the GO-Arg (Arg: arginine) during the ring-opening/closing synthetic sequence.

Introduction

The valorization of CO₂ into medium-to-long term organic vectors is an ongoing *hot-topic* research that is receiving growing attention towards circular carbon economy.^[1] CO₂ is a non-flammable, abundant and cheap organic compound that would represent an ideal C1-organic synthon for the generation of chemical commodities.^[2] Remarkably, state-of-the-art for the industrial CO₂ valorization accounts for a very *focused and narrow* chemical space, with more than 90% of the market related to the synthesis of bio-fuels (*i.e.* MeOH) and agrochemical ingredients (*i.e.* urea).^[3]

In order to expand the current chemical portfolio based on CO₂ valorization, numerous efforts have been devoted by the chemical community, resulting into a wide range of redox-active as well as redox-neutral carbonylative and carboxylative transformations. Among others, one of the most largely scaled production (~ 100 kton/year) regards the covalent incorporation of CO₂ into cyclic organic carbonates.^[4] Cyclic carbonates feature a variety of applications involving the direct use as green solvents, key building blocks for the realization of polyurethanes and direct employment as end-use products such as: lubricants, dyes and coatings.

The ring-expansion of epoxide via CO₂ incorporation relies on a consolidated and accepted mechanistic rationale, featuring a synergistic role of Lewis/Brønsted acids (*i.e.* cationic metal catalysts, strong hydrogen donors) for the epoxide activation that undergoes ring-opening via soft nucleophilic assistance (*i.e.*

halides). In this scenario, numerous protocols have been documented relying on the use of soluble promoters (*i.e.* homogenous conditions).^[5] High efficiency is frequently combined with mild conditions, however, the impossibility to recover the active species negatively impact on the sustainability balance of the overall protocol. In this regard, the search for highly efficient (productivity), sustainable (***mild operative conditions***) and recoverable/re-usable promoters for the commutation of CO₂ into added-value long-term use chemical commodities is still ongoing.

In the light of our current interests on CO₂-based carboxylation reactions^[6] and on the use of graphene oxide (GO) in carbocatalysis,^[7] we envisioned the possibility to realize a robust and recoverable metal-free material for the interconversion of CO₂ into cyclic carbonates. In order to maximize the efficiency of the process we targeted the simultaneous activation of oxiranes and CO₂ by designing a multifunctionalized GO-based composite. In particular, we decided to exploit the GO surface synergistically as a strong H-donor platform (epoxide activation, *vide infra*)^[8] and to bind guanidine-like groups for the nucleophilic activation of carbon dioxide (Figure 1).^[9]

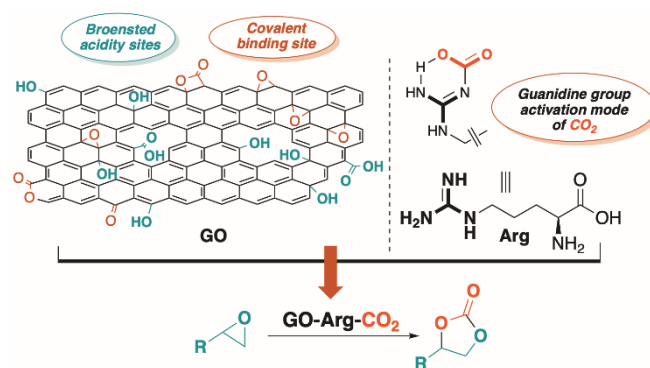


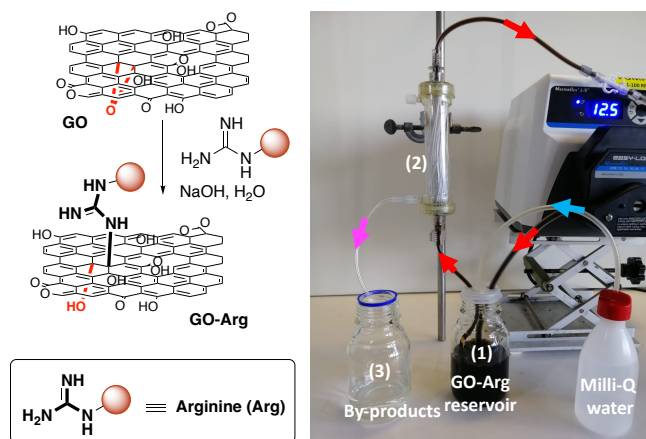
Figure 1. The working idea behind the present methodology.

Focusing on cheap and largely abundant guanidine-containing chemical sources, our attention dropped on the naturally occurring amino acid L-Arginine (Arg) that has been

reported as a valuable CO₂ trapping agent through the formation of arginine-arginine carbamate ion pairs.^[10] Additionally, *L*-Arginine has already found applications as derivatizing agent of inert matrix for the CO₂ trapping/valorization; however, harsh reaction conditions (high temperature and pressure) were required to access synthetically convenient efficiency.^[11] Accordingly, a new gram-scale synthesis of a GO-Arg composite will be described with application in the chemoselective ring-opening of epoxides to cyclic carbonates. Spectroscopic and experimental investigations enabled a full characterization of the material along with a description of the reaction machinery involved.

Results and Discussion

The model GO-Arg hybrid was obtained on gram-scale (2.3 g/batch) via aminative grafting on GO surface under basic conditions (Scheme 1-left, see SI for additional information).^[12] Mechanistically, the ring-opening of the epoxide moieties on GO surface is accounted as most likely during the tagging process.^[13, 14] For purification, we exploited microfiltration on commercial Versatile PES® modules, (Plasmart 100 module, Medica Spa). This procedure is based on the cut-off module (1.000 KDa about 150 nm and with filtering surface of about 0.1 m²) which retains graphene nanosheets but let by-products and unreacted starting materials pass through (Scheme 1-right).^[15] By feeding the module with fresh MilliQ water in loop modalities, the GO-Arg nanosheets are purified and recollected in the reservoir. This unprecedented procedure is fast and less water-energy consuming than the already reported microfiltration-based protocols.



Scheme 1. Left) Synthetic route to GO-Arg, for simplicity only one molecule of arginine was represented. Right) Purification method of GO-Arg by microfiltration in loop-dead end modality [(1): GO-Arg reservoir, (2): purification column via microfiltration on PES® modules, (3): impurity accumulation].

The obtained GO-Arg material was characterized by X-Ray photoelectron spectroscopy (XPS) and attenuated total reflectance infrared spectroscopy (ATR-IR), and its properties compared to those of pristine GO and pristine *L*-arginine (Figure 2, more detail in ESI). XPS analysis of GO-Arg is consistent with the typical structure of this material and is mainly composed of carbon, oxygen and nitrogen, associated to: i) the aromatic sp² regions of GO; ii) C-O/C=O functional groups; and iii) the nitrogen

functional groups (C-N/C=N) present in *L*-Arginine. Since the increase N 1s signal (from 0.7% for pristine GO to 4.9% for GO-Arg) is mainly due to the presence of *L*-Arginine, it is possible to estimate a relative loading of 14% in GO-Arg by considering the atomic ratios of *L*-Arginine (C:N:O = 6:4:2)

Furthermore, the C 1s and N 1s signals of GO-Arg were deconvoluted into its component peaks (see Table S2). From the deconvolution of C 1s signal it is possible to observe the slight increase in the relative amount of carbon sp² (40%) compared to the starting graphene oxide (31%). Unfortunately, most of the nitrogen functional groups (C=N or C-N) present in the GO-Arg are in the same binding energy regions of the oxygenated functional groups. The deconvolution of N 1s signal of GO-Arg presents four distinct components: i) 401.5 eV (6% of N1s) associated to nitrogen already present in GO; ii) 399.8 eV and iii) 400.5 eV associated to different types of nitrogen atoms present in *L*-Arginine (86% of N1s) as reported by Artemenko^[16] and iv) 398.0 eV (8% of N1s) C that was also associated to *L*-Arginine (C=N-C group reported at 398.6 eV).^[17]

ATR-FTIR spectrum of GO-Arg shows the typical O-H stretching of graphene oxide as a broad peak between 3700 and 2500 cm⁻¹. In this region there are also present two peaks at 2924 and 2854 cm⁻¹; these can be ascribed to the asymmetric and symmetric stretching of -CH₂ of the aliphatic chain of arginine. Diagnostic signals appeared also at lower wavenumbers (1650-1550 cm⁻¹, broad peak) that could be associated to the C=C stretching of the graphitic surface and a sharp signal at 1641 cm⁻¹ to the -CO₂H stretching of the tagged arginine.^[18]

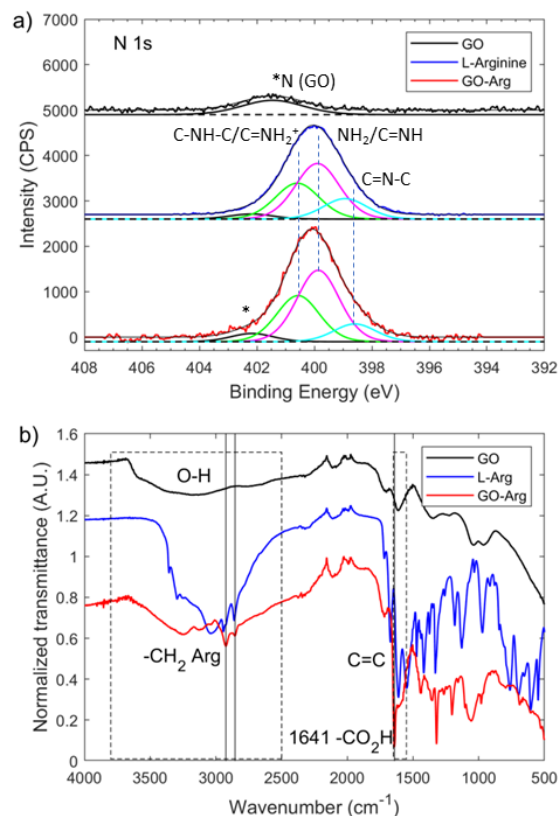



Figure 2. a) High resolution deconvoluted XPS spectra of N 1s peak. b). ATR-IR spectra of GO (black line), GO-Arginine (red line) and *L*-Arginine (blue line).

The GO-Arg material was then employed in the optimization of the reaction conditions through a survey of parameters by adopting the ring-expansion of racemic styrene oxide (**1a**) as a model protocol (Table 1). Temperatures lower than 100 °C were selected in order to prevent the partial GO reduction via thermal releasing of small molecules (*i.e.* CO, CO₂, H₂O) and by degradation of low molecular weight fragments from the carbonaceous matrix.^[19]

Delightfully, the GO-Arg hybrid (160 wt% to **1a**) proved efficiency in promoting the epoxide ring-expansion and delivered the corresponding carbonate **2a** in 77% isolated yield after 24 h at 100 °C (entry 1).^[20] With the aim to optimize the reaction conditions targeting the minimization of material loading, we were pleased to verify that GO-Arg could promote the titled CO₂ fixation in synthetically useful extent (83%) with loading as low as 25 wt% (entry 5). Furthermore, attempts to improve the reaction performance by: i) diluting the reaction mixtures ([**1a**] = 0.1 mM, entry 3) and ii) lowering the GO-Arg loading (10 wt%, entry 6), led to comparable or unsatisfying chemical outcomes with respect to the optimal conditions.

Table 1. Optimization of the reaction conditions.



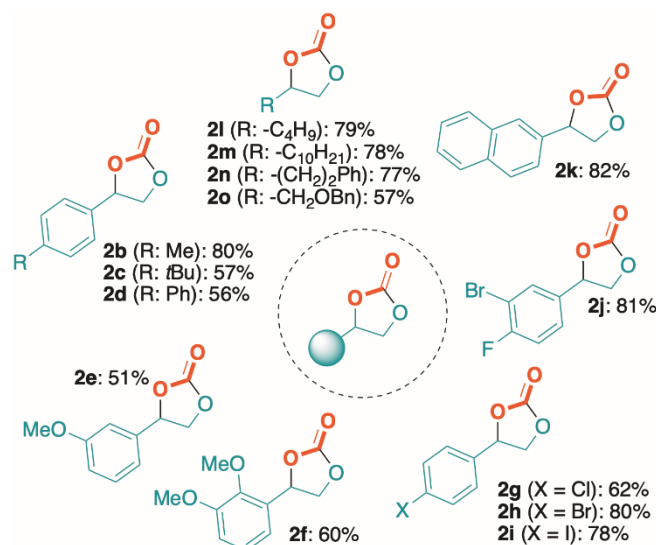
Entry ^[a]	GO-Arg (wt%)	Additives (30 mol%)	conditions	Yield of 2a (%) ^[b]
1	160	TBAI	24 h	77
2	160	TBAI	48 h	86
3	160	TBAI	0.1 mM, 24 h	62
4	60	TBAI	48 h	73
5	25	TBAI	48 h	83
6	10	TBAI	48 h	40
7 ^[c]	25	TBAI ^[c]	48 h	84
8	25	TBAI ^[d]	48 h	75
9	25	--	48 h	--
10 ^[e]	25	TBAI	48 h	--
11	--	TBAI	48 h	12
12	25	TBAI	DMSO, 48 h	67
13	25	TBAI	CH ₃ CN, 48 h	--
14	25	TBAI	Dioxane, 48 h	20
15 ^[f]	60 (GO)	TBAI	48 h	60
16 ^[g]	60 (Arg)	TBAI	48 h	37

[a] All reactions were carried out in dry solvents (0.2 mM, **1a**), additives (30 mol%), unless otherwise specified. [b] isolated yields after flash chromatography. [c] A concentration of **1a** = 0.1 mM was used. [d] 20 mol%. [e] The reaction was carried out under nitrogen atmosphere. [f] GO instead of GO-Arg. [g] L-Arginine instead of GO-Arg. TBAI: tetrabutylammonium iodide.

Blank reactions demonstrated that both TBAI (30 mol%, entry 9) CO₂ atmosphere (entry 10) and GO-Arg (entry 11) were pivotal for the isolation of **2a** (*vide infra* for mechanistic interpretations).

Additionally, DMF was elected as the optimal reaction medium via comparison with other polar organic solvents (entries 12-14). Finally, the present composite GO-Arg proved superior competence with respect to the single components (*i.e.* L-Arg and GO) that provided **2a** in lower extents when utilized independently (yields: 37-60%, entries 15-16). Finally, the genuinely heterogeneous catalysis was circumstantiated by a hot-filtration test that displayed not further advancement in the reaction conversion upon removal of the GO-Arg material after 16 h reaction time (see SI).

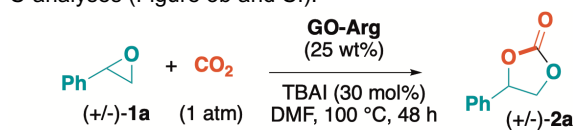
The generality of the methodology was then evaluated by subjecting a range of aromatic (**1b-j**) as well as aliphatic epoxides (**1l-o**) to the ring-expansion protocol, by means of the optimal conditions described in Table 1, entry 5 (Scheme 2). Within the series of aromatic epoxides, we recorded the good to excellent yields (up to 82%) on the corresponding cyclic carbonates regardless both electronic properties and position of the substituents. In addition, aliphatic epoxides turned out to be highly reactive on the optimal conditions yielding the desired cyclic carbonates **2l-o** in good to high isolated yields (up to 79%).



Scheme 2. Scope of the present CO₂ fixation into cyclic carbonates.

The robustness of the functionalized graphene oxide was then considered by assessing both recoverability and reusability of the heterogeneous promoter. In particular, the carbonaceous material was easily separated by the reaction products via centrifugation. Repeated washings with a EtOAc/DMF mixtures enabled the effective removal of the TBAI residues from the solid materials that were finally recovered via dispersion into water and subjected to lyophilization before re-use. With this simple protocol, we were able to recover quantitatively the GO-Arg employed in every run and reuse the material up to 5 consecutive CO₂ fixations providing substantially similar performance both in terms of overall chemical yield (Figure 3a) and kinetic profiles (see SI). The chemical integrity of the GO-Arg surface before and upon

after a catalytic cycle was also verified by C 1s, O 1s and N 1s XPS-analyses (Figure 3b and SI).



a)

Cycle	I	II	III	IV	V
2a (%)	82	78	75	75	74
GO-Arg*	98	98	98	98	98

* % of GO-Arg recovered

b)

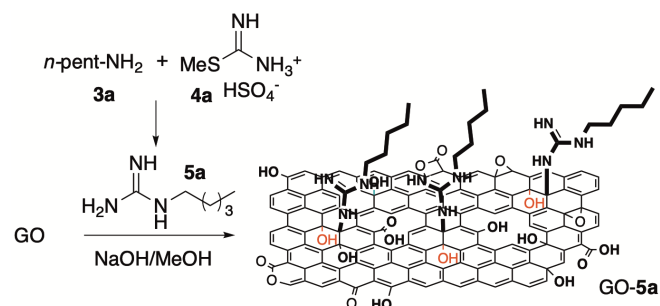
GO-Arg	C (%)	O (%)	N (%)
pristine	73.7	19.6	4.9
I cycle	79.4	15.2	4.4
III cycle	79.8	15.2	4.1
V cycle	80.8	14.3	3.9

XPS analysis (C 1s, O 1s, N 1s)

Figure 3. a) Recycling experiments on the model reaction $1a \rightarrow 2a$. b) Proving the morphological integrity of the GO-Arg composite along the recovering/reuse tests (XPS atomic %). The % of GO-Arg recovered is referred to the amount employed in the previous run.

In particular, the overall chemical surface composition of GO-Arg changed only marginally over the five catalytic cycles accounting for the chemical robustness of the carbo-material in our conditions. Here, the slight reduction observed after the first cycle could be ascribed to an unavoidable partial de-oxygenation of GO upon repeated thermal treatments.^[21] This loss did not seem to involve the arginine pendant, given the unchanged nitrogen content recorded. Additionally, no traces of residual TBAI were identified in the recovered GO-Arg material upon the catalytic iterations.

Therefore, we addressed our efforts towards the comprehension of the activation mode exerted by the polyfunctionalized amino acid pendants (*i.e.* guanidine unit, primary amine) once covalently tagged to the surface of the GO layers. To this purpose, we synthesized *N*-alkylated guanidine **5a** by condensing *S*-methylisothiourea hemisulfate (**4a**) with the *n*-pentyl amine **3a**.^[22] The guanidine derivate **5a** was then implemented in the covalent derivatization of GO, following the synthetic methodology described in the Scheme 3.



Scheme 3. Synthesis of *N*-alkylated guanidine **5a** and implementation in the realization of the composite GO-5a.

The so obtained GO-5a was characterized by X-Ray photoelectron spectroscopy (XPS) and ATR-IR and its properties compared to those of pristine GO and GO-Arg (Figure 4). XPS of GO-5a presented a similar structure compared to GO-Arg. Here, an increase of nitrogen content was observed (3.5%, N 1s at 400.0 eV). Accordingly, a 12% loading of **5a** was estimated by considering the atomic composition of **5a**.

ATR-FTIR spectrum of GO-5a shows the typical O-H stretching vibration peaks of GO (3700 and 2500 cm^{-1}) and two diagnostic peaks at 2924 and 2854 cm^{-1} (absent in GO) that can be ascribed to the stretching of the $-CH_2$ units of the aliphatic chain of **5a**. Finally, the sharp peak at 1641 cm^{-1} , attribute to the carboxyl group stretching in GO-Arg (Figure 2b), here was absent.

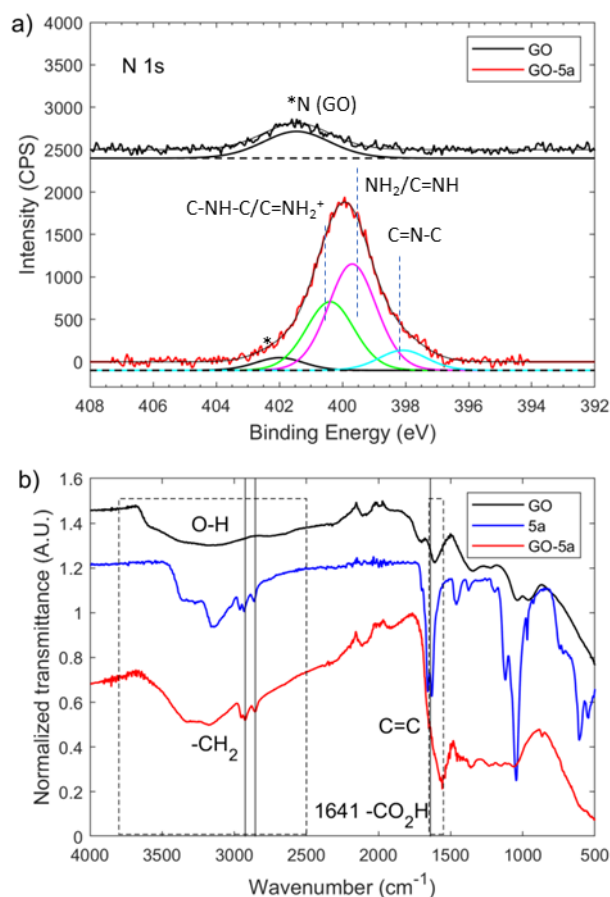


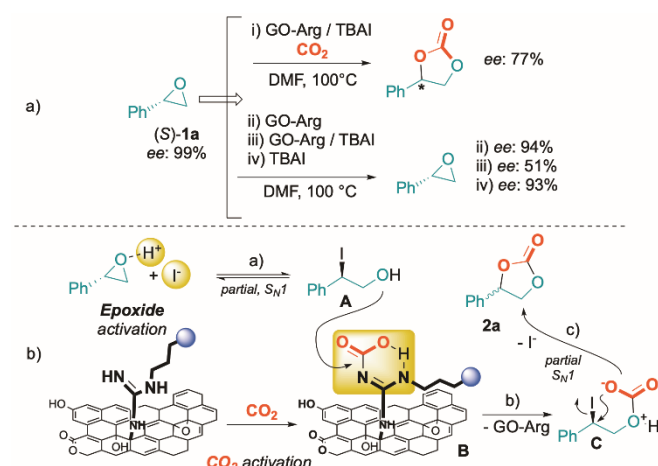
Figure 4. a) High resolution deconvoluted XPS spectra of N 1s peak of GO-5a. b) ATR-IR spectra of pristine GO (black line), GO-5a (red line) and **5a** (blue line).

Interestingly, when GO-5a was utilized in the optimized fixation of CO_2 (Table 1, entry 5), the corresponding cyclic carbonate **2a** was isolated in comparable yield to GO-Arg (88% yield) supporting the pillar “double” role exerted by the guanidyl unit in the present methodology. As a matter of fact, the superbase core is proven to participate in the covalent linking of the GO surface and in the transient activation of CO_2 . On the contrary, the present experimental and spectroscopy evidence indicate the concomitant involvement of the $-NH_2$ group of *L*-Arg on the catalytic process unlikely or at least non predominant.

Finally, some preliminary control experiments were carried out on enantiomerically pure styrene oxide (*S*)-**1a**, providing

important insights to formulate a tentative reaction picture (Scheme 4).

In particular, when the methodology was adapted to enantiomerically pure styrene oxide (*S*)-**1a** the corresponding carbonate **2a** was isolated with substantial racemization (*ee* = 77%, Scheme 4a-i). Intrigued by this partial loss of stereochemical information, some dedicated experiments in the absence of CO₂ were carried out to locate the racemizing step on the mechanistic profile. Here, while GO-Arg and TBAI alone led to the recovery of (*S*)-**1a** with negligible racemization (*ee* = 94% and 93%, respectively), stirring (*S*)-**1a** in the presence of a mixture of GO-Arg and TBAI (DMF, 100 °C, 16 h) caused a significant drop in the enantiomeric excess of the oxirane (*ee* = 51%).



Scheme 4. a) Mechanistic control experiments on enantiopure styrene oxide; b) Pictorial mechanistic sketch of the present CO₂ fixation reaction.

With this information in hand, some mechanistic conclusions can be drawn. In particular, both the iodide anion and the Brønsted acidity released by GO in solution are involved in the initial ring-opening stage a) Scheme 4b. This step resulted reversible through a partial S_N1 profile, as testified by the observed racemization of **1a** under CO₂-free conditions. Therefore, the resulting α-iodo-alkoxide intermediate **A** can trap one molecule of CO₂ previously activated by the guanidyl group of the GO-Arg composite **B**. Finally, the carbonate releasing by intermediate **C** will occur by means of an intramolecular iodide displacement reaction. The partial racemization recorded with enantiopure **1a** suggests that either steps a) and or c) could feature a not negligible S_N1 profile.^[5a] Although the activation of CO₂ by physisorption phenomena could likely parallel the herein proposed covalent interaction (**B**), previously reported covalent activation modes of carbon dioxide on similar amino-functionalized materials prompted us to propose the formation of transient carbonates as key intermediates of the process.^[23]

Conclusion

In the present work we have documented a convenient synthesis and purification of GO-guanidine hybrids to be implemented in the valorization of CO₂ into cyclic carbonates. A range of aliphatic as well as aromatic carbonates were successfully isolated in good yield (up to 85%) under relatively mild conditions. Robustness of the arginine-containing GO was proved via re-iterative runs and by spectroscopic analysis on the

recovered materials. Dedicated control experiments enabled to get insight into the key role of the guanidine group both as a tagging unit and CO₂ activator. Additionally, the observed partial racemization using enantiopure styrene oxide (*S*)-**1a** proposes an epoxide ring-opening step at the more substituted site of the oxirane through a sequence of partial S_N1-type events. Studies towards the implementation of these preliminary findings into CO₂-capture-and-utilization (CCU) modalities are currently under way in our laboratory and will be presented in due course.

Experimental section

In a heat-gun dried screw-capped Schlenk flask, equipped with a magnetic stirring bar and under N₂ atmosphere, GO-Arg (5.0 mg) was added. The tube was evacuated and backfilled with CO₂ (three times). Anhydrous DMF (1.0 mL) was then added and bubbled for 1 minute under a flow of CO₂. Then, **1** (0.2 mmol, 1 equiv.) and TBAI (22.0 mg, 0.06 mmol, 30 mol%) were added. The tube was then sealed and placed in an oil bath at 100 °C where it was vigorously stirred for 48 h. After cooling to room temperature, the reaction mixture was filtered through a Celite pad to remove GO-Arg, washing with EtOAc (3 x 5 mL). The solvents were removed under reduced pressure (rotary evaporator then high-vacuum pump to remove DMF) and the residue was purified by flash column chromatography (FC) on silica gel (*n*-hex/EtOAc mixtures) to afford pure products **2**.

Acknowledgements

We are grateful to the University of Bologna for financial support and PRIN-2017 project 2017W8KNZW. The authors gratefully acknowledge the support of this work through the projects 825207-GO-FOR-WATER, 881603-GrapheneCore3-SH-GRAPHIL, LIFE20 ENV/IT/001001 Life-Remembrance and Dr L. Bocchi, and M. Fecondini (Medica SpA) for providing Plasmart microfiltration cartridges. MB is also grateful to Consorzio CINMPIS.

Keywords: Carbon dioxide • Epoxide • Graphene oxide • Arginine • Organic carbonate

- [1] M. Aresta, A. Dibenedetto, *Front. Energ. Res.* **2020**, *8*, art 159.
- [2] a) Q. Liu, L. Wu, R. Jackstell, M. Beller, *Nat. Commun.* **2015**, *6*, 5933; b) P. Gabrielli, M. Gazzani, M. Mazzotti, *Ind. Eng. Chem. Res.* **2020**, *59*, 7033-7045.
- [3] X. Zhang, G. Zhang, C. Song, X. Guo, *Front. Energ. Res.* **2021**, *8*, art. 621119.
- [4] P.P. Pescarmona, *Curr. Opin. Green Sustain. Chem.* **2021**, *29*, 100457.
- [5] a) R. Dalpozzo, N. Della Cà, B. Gabriele, R. Mancuso, *Catalysis* **2019**, *9*, 511; b) L. Guo, K.J. Lamb, M. North, *Green Chem.* **2021**, *23*, 77-118.
- [6] a) A. Cerveri, S. Pace, M. Monari, M. Lombardo, M. Bandini, *Chem. Eur. J.* **2019**, *25*, 15272-15276; b) A. Cerveri, R. Giovanelli, D. Sella, R. Pedrazzani, M. Monari, O. Nieto Faza, C. Silva López, M. Bandini, *Chem. Eur. J.* **2021**, *27*, 7657-7662; c) L. Lombardi, A. Cerveri, L. Ceccon, R. Pedrazzani, M. Monari, G. Bertuzzi, M. Bandini, *Chem. Commun.* **2022**, *58*, 4071-4074; d) For a review article see: G. Bertuzzi, A. Cerveri, L. Lombardi, M. Bandini, *Chin. J. Chem.*, **2021**, *39*, 3116-3126.

- [7] a) L. Favaretto, J. An, M. Sambo, A. De Nisi, C. Bettini, M. Melucci, A. Kovtun, A. Liscio, V. Palermo, A. Bottoni, F. Zerbetto, M. Calvaresi, M. Bandini, *Org. Lett.* **2018**, *20*, 3705-3709; b) L. Lombardi, D. Bellini, A. Bottoni, M. Calvaresi, M. Monari, A. Kovtun, V. Palermo, M. Melucci, M. Bandini, *Chem. Eur. J.* **2020**, *26*, 10427-10432; c) L. Lombardi, A. Kovtun, S. Mantovani, G. Bertuzzi, L. Favaretto, C. Bettini, V. Palermo, M. Melucci, M. Bandini, *Chem. Eur. J.* **2022**, e202200333.
- [8] a) D. R. Dreyer, C. W. Bielawski, *Chem. Sci.* **2011**, *2*, 1233-1240; b) D. Haag, H.H. Kung, *Top. Catal.* **2014**, *57*, 762-773; c) C.K. Chua, M. Pumera, *Chem. Eur. J.* **2015**, *21*, 12550-12562; d) D. Deng, K.S. Novoselov, Q. Fu, N. Zheng, Z. Tian, X. Bao, *Nature Nanotech.* **2016**, *11*, 218-230; e) D. S. Su, G. Wen, S. Wu, F. Peng, R. Schlägl, *Angew. Chem. Int. Ed.* **2017**, *56*, 936-964; f) X. Duan, H. Sun, S. Wang, *Acc. Chem. Res.* **2018**, *51*, 678-687; g) M. Antonietti, N. Lopez-Salas, A. Primo, *Adv. Mat.* **2019**, *31*, 1805719; h) C. Campisciano, M. Gruttadauria, F. Giacalone, *Chem.Cat.Chem.* **2019**, *11*, 90-113; i) L. Lombardi, M. Bandini, *Angew. Chem., In. Ed.* **2020**, *59*, 20767-2078; j) A. Jiřicková, O. Jankovský, Z. Sofer, D. Sedmidubský, *Materials*, **2022**, *15*, 920.
- [9] a) S.Y. Huang, J. Ma, J.P. Li, N. Zhao, W. Wei, Y.H. Sun, *Catal. Commun.* **2008**, *9* 276-280; b) J. Ma, X. Zhang, N. Zhao, A.S.N. Al-Arifi, T. Aouak, Z. A. Al-Othman, F. Xiao, W. Wei, Y. Sun, *J. Mol. Cat. A: Chem.* **2010**, *315*, 76-81; c) H. M. Lee, I. S. Youn, M. Saleh, J.W. Lee, K.S. Kim, *Phys. Chem. Chem. Phys.* **2015**, *17*, 10925-10933; d) For general review see: S.P. Sreejyothi, S.K. Mandal, *Chem. Sci.* **2020**, *11*, 10751-10593.
- [11] C. Cheng, H. Shen, N.-N. Shen, C. Castro, V. Dubovoy, D. Wu, R. Subramanyan, X.-Y. Huang, C.E. Pitsch, X. Wang, L. Pan, *Ind. Eng. Chem. Res.* **2021**, *60*, 17745-17749.
- [12] a) N. Hsan, P.K. Dutta, S. Kumar, J. Koh, *J. CO₂ Util.* **2022**, *59*, 101958. For examples of amino and metal functionalized GO/rGO with implications on CO₂ conversion into cyclic epoxides and carbamates, see: b) V.B. Saptal, T. Sasaki, K. Harada, D. Nichio-Hamane, B.B. Bhanage, *ChemSusChem* **2016**, *9*, 644-650 and c) X. Zhang, K.-H. Chen, Z.-H. L.-N. He, *ChemCatChem* **2020**, *12*, 4825-4830.
- [13] S. Khabnadideh, E. Mirzaei, L. Amiri-Ziretol, *J. Mol. Struct.* **2022**, *1261*, 132934.
- [14] I.A. Vacchi, C. Spinato, J. Raya, A. Bianco, C. Ménard-Moyon, *Nanoscale*, **2016**, *8*, 13714-13721.
- [15] a) S. Mantovani, S. Khaliha, L. Favaretto, C. Bettini, A. Bianchi, A. Kovtun, M. Zambianchi, M. Gazzano, B. Casentini, V. Palermo, M. Melucci, *Chem. Commun.* **2021**, *57*, 3765-3768; b) S. Mantovani, S. Khaliha, T. D. Marforio, A. Kovtun, L. Favaretto, F. Tunioli, A. Bianchi, G. Petrone, A. Liscio, V. Palermo, M. Calvaresi, M.L. Navacchia, M. Melucci *Chem. Commun.* **2022**, *58*, 9766-9769.
- [16] A. Artemenko, A. Shchukarev, P. Štenclová, T. Wågberg, J. Segervald, X. Jia, A. Kromka, *IOP Conf. Series: Materials Science and Engineering*, **2021**, *1050*, 012001
- [17] R.A. Zangmeister, T.A. Morris, M.J. Tarlov, *Langmuir*, **2013**, *29*, 8619-8628.
- [18] B. Wu, L. Zhang, B. Jiang, Q. Li, C. Tian, Y. Xie, W. Li, H. Fu, *Angew. Chem. Int. Ed.* **2021**, *60*, 4815-4822.
- [19] S. Zhang, H. Zhang, F. Cao, Y. Ma, Y. Qu, *ACS Sust. Chem. Eng.* **2018**, *6*, 4204-4211.
- [20] The CO₂ internal pressure of the reaction vessels was estimated as ca. 1.25 atm based on the upper volume of the reactor.
- [21] S. Eigler, C. Dotzer, A. Hirsch, M. Enzelberger, P. Müller, *Chem. Mat.* **2012**, *24*, 1276-1282.
- [22] F. Z. Liu, H. Fang, W. F. Xu, *Chin. Chem. Lett.* **2007**, *18*, 393-396.
- [23] a) J. Cai, J. Chen, P. Zeng, Z. Pang, X. Kong, *Chem. Mat.* **2019**, *31*, 3729-3735; b) W.-H. Xie, X. Yao, H. Li, H.-R. Li, L.-N. He, *ChemSusChem* **2022**, *15*, e202201004.

